# A COMPARISON OF INTENSE ELECTROSTATIC WAVES NEAR $f_{UHR}$ WITH LINEAR INSTABILITY THEORY

W. S. Kurth[1], M. Ashour-Abdalla[2], L. A. Frank[1], C. F. Kennel[3], D. A. Gurnett[1], D. D. Sentman[4], and B. G. Burek[1]

[1] Department of Physics and Astronomy, The University of Iowa, Iowa City, IA 52242

[2] Department of Physics and Institute of Geophysics and Planetary Physics, University of California, Los Angeles, CA 90024

[3] Department of Physics, Institute of Geophysics and Planetary Physics, and Center for Plasma Physics and Fusion Engineering, University of California, Los Angeles, CA 90024

[4] Institute of Geophysics and Planetary Physics, University of California, Los Angeles, CA 90024

*Abstract.* Intense electrostatic waves beyond the plasmapause have recently been identified at frequencies near the upper hybrid resonance frequency. In addition, the waves occur within a band at an odd, half-harmonic of the local electron gyrofrequency. These bands of electrostatic turbulence are among the most intense waves detected within the earth's magnetosphere. Measurements obtained with the ISEE 1 plasma wave receiver show that the intense waves appear to be intensifications of an electrostatic cyclotron harmonic band near the upper hybrid resonance frequency. A straightforward explanation of intense waves at the upper hybrid resonance frequency exists in the electrostatic multi-cyclotron emission theory. For a broad range of plasma parameters nonconvective instability or large spatial growth rates occur within the cyclotron band encompassing the cold upper hybrid frequency. Comparison of spatial growth rate spectra with measured wave spectra shows that there is excellent qualitative agreement between the linear theory and the observed wave characteristics.

## Introduction

Intense electrostatic waves near the upper hybrid resonance frequency, $f_{UHR}$, have been detected near but beyond the plasmapause between ±50° magnetic latitude at all local times [*Kurth et al.*, 1979]. The waves detected by plasma wave receivers on board Hawkeye 1 and IMP 6 had amplitudes between 1 and 20 mV m$^{-1}$ and bandwidths typically less than 10% of the center frequency. The waves were shown to intensify when $f_{UHR} \simeq (n + \frac{1}{2})f_g^-$, where $f_g^-$ is the electron gyrofrequency. Their electric fields were found to be nearly perpendicular to the geomagnetic field, consistent with upper hybrid modes.

An example of upper hybrid waves from the ISEE 1 sweep frequency receiver [*Gurnett et al.*, 1978] is shown in Figure 1. Wave intensity, denoted by shading with darker areas representing higher intensities, is displayed as a function of frequency and time. The band found near 400 kHz at 2230 UT, which decreases in frequency with increasing radial distance, R, is near $f_{UHR}$. $f_{UHR}$ abruptly decreases at the plasmapause at about 2125 UT. The band continues into the outer magnetosphere near the low frequency cutoff of the nonthermal continuum radiation, which appears as diffuse wave activity generally above 20 kHz. The peak intensity of the $f_{UHR}$ band occurs at about 2110 UT near 30 kHz with an electric field strength of about 7 mV m$^{-1}$. The dark rectangular region is the result of receiver saturation due to the intense band. (The quoted field strength was obtained from another portion of the receiver unaffected by saturation.) During the event the spacecraft was at about 6.9° magnetic latitude, 12.7 hours magnetic local time, and 5.5 $R_E$ radial distance. The weak banded emissions below the continuum radiation are diffuse electrostatic bands with $f \simeq (n + \frac{1}{2})f_g^-$ and amplitudes near 1 $\mu$V m$^{-1}$. The intensification at 2110 UT appears to occur when the $9f_g^-/2$ band merges with the $f_{UHR}$ band.

Figure 2 presents data from an outbound pass of ISEE 1 which reveal weak, diffuse electrostatic bands between the first five gyroharmonics. As in Figure 1, $f_{UHR}$ follows the lower cutoff of the continuum radiation at approximately 15 kHz. The waves intensify at each point of intersection where $(n + \frac{1}{2})f_g^- \simeq f_{UHR}$. There appear to be stop bands between each intensification.

Simultaneous wave and plasma measurements on board Hawkeye revealed a suggestive correlation between intense electrostatic wave events and 1-20 keV electron intensities [*Kurth et al.*, 1979]. Near the geomagnetic equator, where the Hawkeye Lepedea could sample a broad range of pitch angles, virtually all events were accompanied by anisotropic distributions of few-keV electrons whose intensities peaked at pitch angles near 90°. *Kurth et al.* [1979] demonstrated the existence of at least two possible sources of free energy; temperature anisotropy, and a loss-cone distribution, that might drive the $f_{UHR}$ instability. The possibility of a bump-on-tail free-energy source was also suggested. *Rönnmark et al.* [1978] have also reported a loss-cone distribution associated with a relatively intense $f_{UHR}$ event.

Figure 3 shows a contour plot of the electron distribution obtained by the ISEE 1 quadrispherical Lepedea [*Frank et al.*, 1978] at the same time as the intense UHR band in Figure 1. There is little evidence of a loss cone in this distribution function, but there is a distinct temperature anistropy, $A = (T_\perp / T_\parallel - 1)$, of about 0.3. Also, notice the relatively flat $f(v_\perp)$ near $4 \times 10^9$ cm (sec)$^{-1}$. Although the anisotropy may be a candidate source of free energy in the electron velocity distribution function, single component calculations [*Ashour-Abdalla and Cowley*, 1974] indicate that the small measured anisotropy should not destabilize fourth harmonic waves as observed. Detailed analyses of the Lepedea data at pitch angles near 90° and $v_\perp \approx 4 \times 10^9$ cm (sec)$^{-1}$ reveal a minimum in the distribution function which results in a region of positive slope with respect to $v_\perp$. This feature may correspond to the bump-on-tail free-energy source suggested by *Kurth et al.* [1979]. We shall discuss the apparent lack of a loss-cone free-energy source in the Discussion section.

*Kurth et al.* [1978, 1979] have outlined a scenario to explain intense $f_{UHR}$ waves that draws upon the theory of multi-cyclotron harmonic instabilities [*Hubbard and Birmingham*, 1978; *Ashour-Abdalla and Kennel*, 1978a, b; *Ashour-Abdalla et al.*, 1979a, b]. In this paper we first give a qualitative comparison between the observations of Figure 2 and theoretical expectation, and then compare the measured spectral amplitudes for the event of Figure 1 and theoretical calculations of maximum spatial growth rates as a function of frequency. A parallel, but entirely separate comparison of upper hybrid wave amplitudes with multi-cyclotron theory [*Rönnmark et al.*, 1978] generally supports our conclusions.

## Comparison of Multi-Cyclotron Instability Theory With Upper Hybrid Wave Observations

*Ashour-Abdalla and Kennel* [1978a, b] and *Ashour-Abdalla et al.* [1979a, b] have parametrically surveyed the spatial growth rates of multi-harmonic instabilities using an analytic model of

Copyright 1979 by the American Geophysical Union.

Paper number 9L0739.
0094-8276/79/069L-0739$01.00

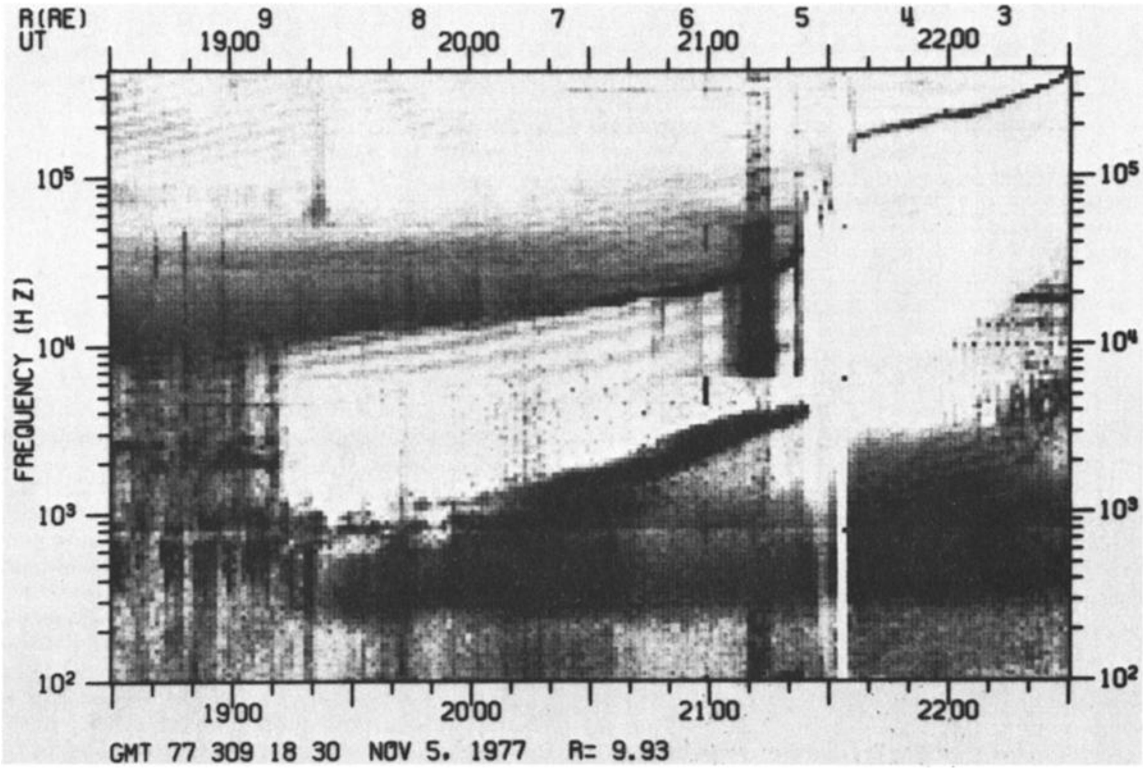


Fig. 1. A frequency-time spectrogram showing intensification of the upper hybrid resonance band when $f_{UHR} \approx 9f_g^-/2$. Weak, diffuse electrostatic bands occur near $(n + ½)f_g^-$ harmonics below $f_{UHR}$.

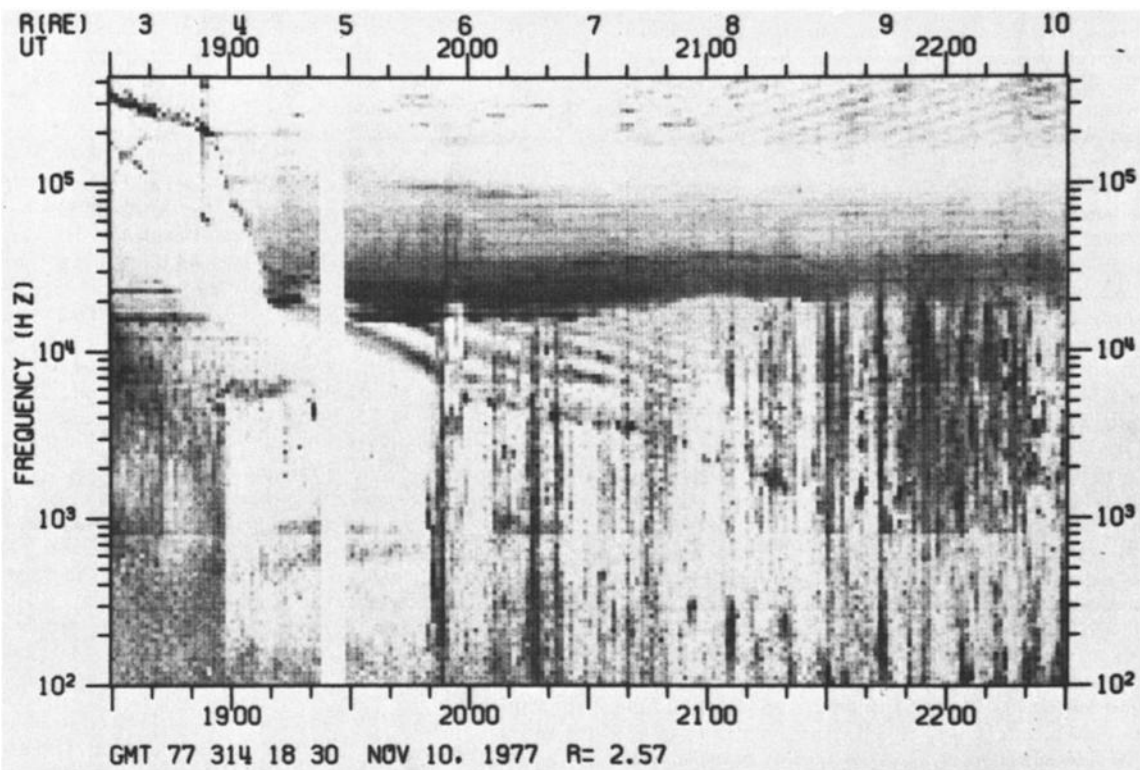


Fig. 2. A frequency-time spectrogram showing intensifications when $f_{UHR} \approx (n + ½)f_g^-$ for n = 1, 2, 3, 4, and 5. Notice that as each diffuse band intersects the lower cutoff of the continuum radiation near $f_{UHR}$ there is an intensification. There are also stop bands between the intensifications as $f_{UHR}$ moves from one harmonic band to the next.

the electron distribution. This model consists of a hot electron distribution, with a loss-cone free-energy source and a cold electron distribution. The free parameters are the strength of the loss-cone feature, the hot and cold densities, $n_h$ and $n_c$, and temperatures $T_h$ and $T_c$. Using this model of the electron distribution, we have calculated the regions of nonconvective instability, NCI, for the first four harmonic bands displayed in Figure 4 as a function of $n_c/n_h$ and $f_{UHC}/f_g^-$, where $f_{UHC}$ is the cold upper hybrid frequency. The curves were constructed by searching in wave-number space for the maximum spatial growth rate $K_i$, assuming $T_c/T_h = 5 \times 10^{-2}$. If the group velocity is zero when the temporal growth rate is positive, a nonconvective instability is possible. Since the waves propagate only slowly, if at all, out of their amplification region, they could reach large amplitudes.

Near the plasmapause, we expect $n_c/n_h > 1$ and, therefore, $f_{UHR} \simeq f_{UHC}$. Figure 4 indicates that when $n_c/n_h \gtrsim 1.6$, NCI occurs only in the harmonic band encompassing $f_{UHC}$. Convective growth or damping occurs at other frequencies. Moreover, there are stop bands between each region of NCI. The widths in $f_{UHC}/f_g^-$ of the NCI regions and the interspersed stop bands depend upon $T_c/T_h$ and the strength of the loss-cone distribution, and may vary. However, the qualitative behavior is general. For example, stop bands are expected because of strong damping at cyclotron harmonics. We note that the successive appearance of intense emissions each time $f_{UHR}$ intersects $(n + \frac{1}{2})f_g^-$ revealed in Figure 2 is qualitatively consistent with Figure 4.

The intense waves near the intersection of $f_{UHR}$ and $(9/2)f_g^-$ of Figure 1 would be consistent with Figure 4, if $4 < f_{UHC} < 5$ and $1.6 < n_c/n_h < 8$. For these parameters, Figure 4 predicts rapid growth for the fourth, or $9f_g^-/2$, band. Other bands in Figure 1 are weak, consistent with the hypothesis that convective instabilities may not reach as large amplitudes as those which are nonconvective.

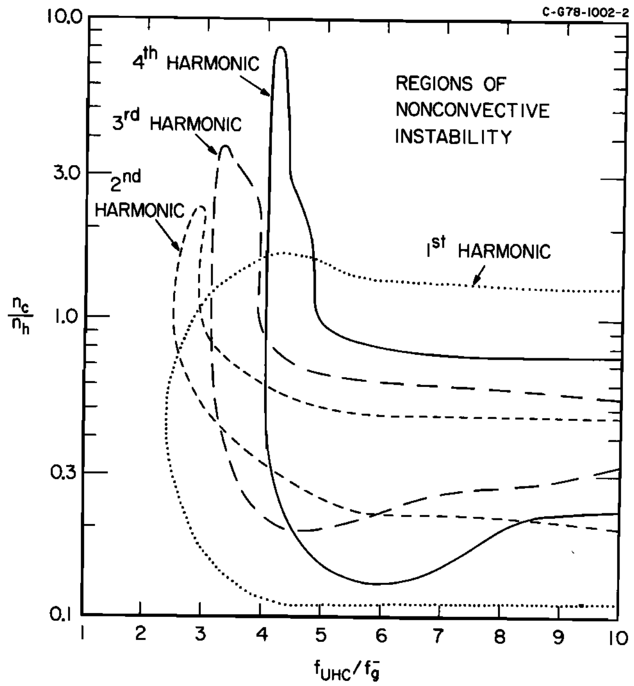


Fig. 4. Regions of nonconvective instability for the first four harmonic bands. Notice that for regions generally above $n_c/n_h = 1.6$ individual bands may become nonconvectively unstable and could produce intense waves in the band including $f_{UHC}$ with weak, convective growth in the lower frequency bands.

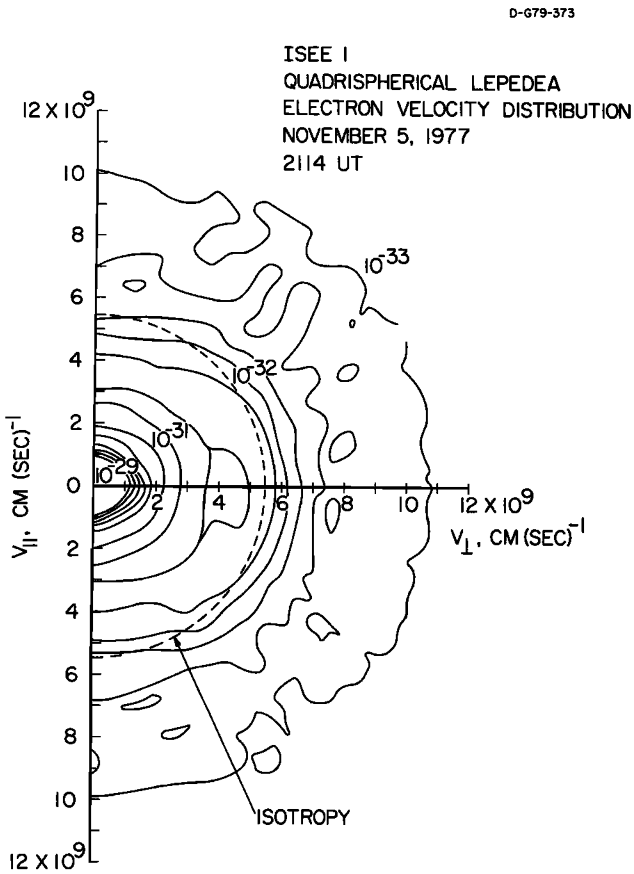


Fig. 3. Contours of $f(v_\perp, v_\parallel)$ for the time period when intense waves at $f_{UHR}$ are present in Figure 1. Two possible sources of free energy are the temperature anisotropy and a region of positive slope in f near $4 \times 10^9$ cm (sec)$^{-1}$ at 90° pitch angle.

Figure 5 directly compares the measured spectral amplitudes corresponding to the intense event in Figure 1 with calculated spatial growth rates as a function of frequency. Since the temporal growth rate and group velocity depend strongly on $K_\perp/K_\parallel$, growth rates calculated at constant wave number are not sufficient. Hence, a search of wave-number space for the maximum spatial growth rate as a function of frequency is necessary. Under normal conditions, the plasma wave receiver response is largest for the most intense wave.

In the upper panel of Figure 5, the spectral density of the event in Figure 1 is shown as a function of $f/f_g^-$ taken at a time prior to receiver saturation, but when the $f_{UHR}$ band was still intense. ISEE 1 magnetometer measurements provided the magnetic field to calculate $f_g^-$ [*C. T. Russell*, private communication, 1978]. The lower panel displays the spatial growth rate $K_i$, normalized to the hot electron Larmor radius $\rho_h$, as a function of $f/f_g^-$. We chose $n_c/n_h = 3$, $T_c/T_h = 5 \times 10^{-2}$, and $f_{UHC} = 4.5 f_g^-$. There is qualitative agreement between observation and theory. The lower three bands, which have low amplitudes in the upper panel, also have weak convective growth rates. The strong fourth harmonic band seen in the upper panel corresponds to the strong calculated spatial growth displayed in the lower panel. The bandwidths are in general agreement.

## Discussion

Electrostatic waves observed with the ISEE 1 plasma wave receiver near $f_{UHR}$ qualitatively agree with a linear theory of multi-cyclotron harmonic emissions. The peak amplitudes and bandwidths observed are similar to those calculated for maximum spatial growth rates. Measurements on Hawkeye [*Kurth et al.*, 1979] of similar waves suggest that the electric field polarization is also consistent with theory.

Perhaps the most interesting point of our comparison of observations and theory is the open question of what features in the

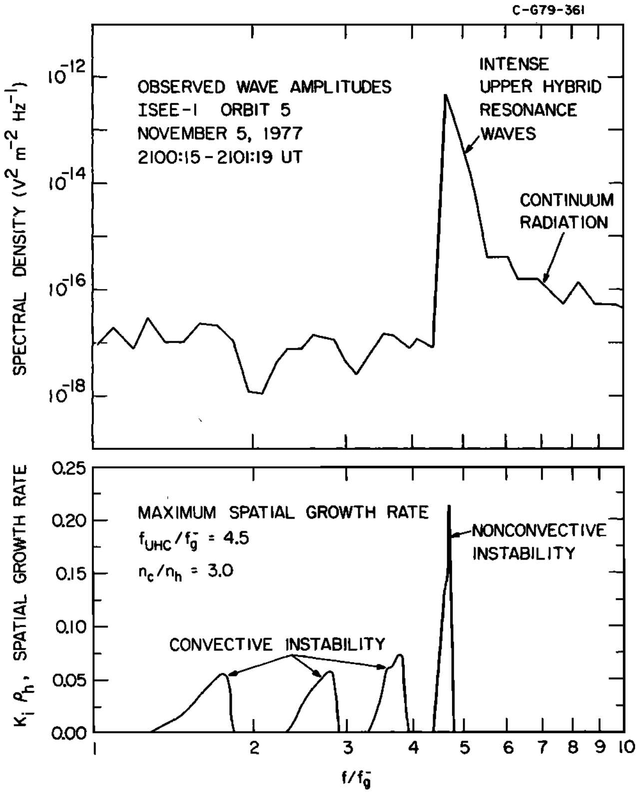


Fig. 5. A comparison of the measured wave spectrum for the event shown in Figure 1 with the theoretical maximum spatial growth rate spectrum. Notice that there is excellent qualitative agreement. The intense band at the $9f_g^-/2$ harmonic coincides with the large nonconvective growth rates in the fourth band in the lower panel. Weaker wave activity in the lower three harmonic bands corresponds well with the lesser convective growth rates shown in the lower panel.

electron velocity distribution function are directly responsible for the intense waves near $f_{UHR}$. *Rönnmark et al.* [1978] and *Kurth et al.* [1979] have both reported loss-cone distributions in association with the UHR waves and all current theories rely on the loss cone as a free-energy source, yet the distribution in Figure 3 shows only the faintest evidence of such a feature. It is interesting that the distributions observed before and after the most intense UHR band with ISEE 1 and also those observed with ISEE 2 show stronger loss-cone-like features than the distribution in Figure 3. Of course, the very intense electrostatic waves could strongly diffuse the energy and pitch angle distributions and thus fill in any loss cone in a quasilinear manner [*Lyons*, 1974; *Sentman et al.*, 1979]. It is also important to consider alternative free-energy sources, such as temperature anisotropy and/or a local minimum in the distribution function at 90° pitch angle. Even if the electron distributions in the magnetosphere are weakly unstable, the nonconvective nature of this instability may still promote very large wave growth.

Comparison of theory and experiment at a more quantitative level becomes complex from this point on. Great care must be taken not to over interpret the measured distribution function, which presently does not extend below 200 eV. In a two-component theory, the ratio of hot-to-cold densities and temperatures play highly significant roles in determining the spatial growth rates. Thus, knowledge of the form of the low energy electron distribution is not only important to estimate the wave group velocities, but may also reveal additional sources of free energy for wave growth. For example, anisotropies in the cold electrons have been observed in magnetospheric plasmas in association with electron cyclotron harmonic waves [*J. J. Sojka*, private communication, 1979].

It is still necessary to investigate thoroughly the role of cold electrons associated with the intense upper hybrid waves. This study will be carried out using the ISEE quadrispherical Lepedea when it is configured to measure electrons in the energy range extending to 1 eV. To estimate the possible significance of a colder component than those electrons shown in Figure 3 we have performed sample calculations using a three-component distribution (i.e., cold, warm, and hot electrons). We found our qualitative results depended primarily upon the warm and hot components. Similar conclusions have been independently reached by *Rönnmark et al.* [1978]. Therefore, the parameter searches presented here are probably qualitatively reasonable. Nonetheless, detailed comparison with theory awaits measurements of these lower energy electrons.

Moreover, the comparison of the amplitudes of the waves, which surely are in a saturated state, with linear instability theory can only be of a qualitative nature. While linear theory probably can reliably produce the frequencies of peak amplitudes, and the overall unstable bandwidth, the propagation and nonlinear saturation of the waves must be understood before the spectrum can be calculated.

Acknowledgements. The authors wish to thank C. T. Russell for providing the ISEE 1 magnetic field measurements used in Figure 5, and W. Livesey for his industry in plotting the contours in Figure 4.

The research at The University of Iowa was supported by NASA under Contracts NAS5-20093 and NAS5-20094 from Goddard Space Flight Center and Grant NGL-16-001-043. The research at the University of California at Los Angeles was supported by NASA Grant NGL-05-007-190, NSF Grant ATM-76-13792, and University of Iowa Subcontract R44855.

## References

Ashour-Abdalla, M., and S. W. H. Cowley, Wave-particle interactions near the geostationary orbit, in *Magnetospheric Physics*, ed. by B. M. McCormac, D. Reidel, Dordrecht, Netherlands, 1974.

Ashour-Abdalla, M., and C. F. Kennel, Nonconvective and convective electron cyclotron harmonic instabilities, *J. Geophys. Res.*, *83*, 1531, 1978a.

Ashour-Abdalla, M., and C. F. Kennel, Multi-harmonic electron cyclotron instabilities, *Geophys. Res. Lett.*, *5*, 711, 1978b.

Ashour-Abdalla, M., C. F. Kennel, and W. Livesey, A parametric study of multiharmonic instabilities in the magnetosphere, *J. Geophys. Res.*, in press, 1979a.

Ashour-Abdalla, M., C. F. Kennel, and D. D. Sentman, Magnetospheric multi-harmonic instabilities, in *Astrophysics and Space Science Book Series*, ed. by P. J. Palmadesso, D. Reidel, Dordrecht, Netherlands, 1979b.

Frank, L. A., D. M. Yeager, H. D. Owens, K. L. Ackerson, and M. R. English, Quadrispherical Lepedeas for ISEE's-1 and -2 plasma measurements, *Geoscience Electronics*, *GE-16*, 221, 1978.

Gurnett, D. A., F. L. Scarf, R. W. Fredricks, and E. J. Smith, The ISEE-1 and ISEE-2 plasma investigation, *Geoscience Electronics*, *GE-16*, 225, 1978.

Hubbard, R. F., and T. J. Birmingham, Electrostatic emissions between electron gyroharmonics in the outer magnetosphere, *J. Geophys. Res.*, *83*, 4837, 1978.

Kurth, W. S., M. Ashour-Abdalla, D. A. Gurnett, and C. F. Kennel, A comparison of intense electrostatic waves observed beyond the plasmapause with linear instability theory, *EOS Trans. AGU*, *59*, 1156, 1978.

Kurth, W. S., J. D. Craven, L. A. Frank, and D. A. Gurnett, Intense electrostatic waves near the upper hybrid resonance frequency, *J. Geophys. Res.*, in press, 1979.

Lyons, L. R., Electron diffusion driven by magnetospheric electrostatic waves, *J. Geophys. Res.*, *79*, 575, 1974.

Rönnmark, K., H. Borg, P. J. Christiansen, M. P. Gough, and D. Jones, Banded electron cyclotron harmonic instability—a first comparison of theory and experiment, *Space Sci. Rev.*, *22*, 401, 1978.

Sentman, D. D., L. A. Frank, C. F. Kennel, D. A. Gurnett, and W. S. Kurth, Electron distribution functions associated with electrostatic emissions in the dayside magnetosphere, *U. of California Res. Report PPG-410*, University of California, Los Angeles, 1979.

(Received April 17, 1979;
accepted May 10, 1979.)